Disrupting phosphatase SHP2 in macrophages protects mice from high-fat diet-induced hepatic steatosis and insulin resistance by elevating IL-18 levels

Received for publication, November 9, 2019, and in revised form, June 10, 2020 Published, Papers in Press, June 16, 2020, DOI 10.1074/jbc.RA119.011840

Wen Liu[1,‡], Ye Yin[2,‡], Meijing Wang[1,‡], Ting Fan[1], Yuyu Zhu[1], Lihong Shen[1], Shuang Peng[1], Jian Gao[1], Guoliang Deng[1], Xiangbao Meng[3], Lingdong Kong[1], Gen-Sheng Feng[4], Wenjie Guo[1,*], Qiang Xu[1,*], and Yang Sun[1,5,6,*]

From the [1]State Key Laboratory of Pharmaceutical Biotechnology, Department of Biotechnology and Pharmaceutical Sciences, School of Life Sciences, Nanjing University, Nanjing, China, [2]Key Laboratory of Human Functional Genomics of Jiangsu Province, Department of Biochemistry and Molecular Biology, Nanjing Medical University, Nanjing, China, [3]State Key Laboratory of Natural and Biomimetic Drugs, Department of Chemical Biology, School of Pharmaceutical Sciences, Peking University, Beijing, China, [4]Department of Pathology and Division of Biological Sciences, University of California San Diego, La Jolla, California, USA, [5]State Key Laboratory of Drug Research, Shanghai Institute of Materia Medica, Chinese Academy of Sciences, Shanghai, China, and [6]Chemistry and Biomedicine Innovation Center (ChemBIC), Nanjing University, Nanjing, China

Edited by Jeffrey E. Pessin

Chronic low-grade inflammation plays an important role in the pathogenesis of type 2 diabetes. Src homology 2 domain-containing tyrosine phosphatase-2 (SHP2) has been reported to play diverse roles in different tissues during the development of metabolic disorders. We previously reported that SHP2 inhibition in macrophages results in increased cytokine production. Here, we investigated the association between SHP2 inhibition in macrophages and the development of metabolic diseases. Unexpectedly, we found that mice with a conditional SHP2 knockout in macrophages (cSHP2-KO) have ameliorated metabolic disorders. cSHP2-KO mice fed a high-fat diet (HFD) gained less body weight and exhibited decreased hepatic steatosis, as well as improved glucose intolerance and insulin sensitivity, compared with HFD-fed WT littermates. Further experiments revealed that SHP2 deficiency leads to hyperactivation of caspase-1 and subsequent elevation of interleukin 18 (IL-18) levels, both *in vivo* and *in vitro*. Of note, IL-18 neutralization and caspase-1 knockout reversed the amelioration of hepatic steatosis and insulin resistance observed in the cSHP2-KO mice. Administration of two specific SHP2 inhibitors, SHP099 and Phps1, improved HFD-induced hepatic steatosis and insulin resistance. Our findings provide detailed insights into the role of macrophagic SHP2 in metabolic disorders. We conclude that pharmacological inhibition of SHP2 may represent a therapeutic strategy for the management of type 2 diabetes.

The marked increase in the incidence of type 2 diabetes (T2D) has made this disease one of the major threats to global health. T2D is caused by several pathophysiologic mechanisms, but obesity is recognized as a factor that contributes to insulin resistance, one of the defining clinical features in metabolic syndrome (1, 2). Obesity gives rise to a state of chronic, low-grade inflammation, and recent studies in humans and mice have shown that obesity and inflammation are highly integrated processes in the pathogenesis of insulin resistance, T2D, and nonalcoholic fatty liver disease (NAFLD) (3–5).

Increasing evidence now implicates cytokines in the development of metabolic disease, given their roles in the regulation of energy homeostasis (6). One cytokine, IL-1β, is a key mediator of the inflammatory response and contributes to ectopic fat accumulation in hepatocytes and macrophage infiltration in adipose tissue (7). Lack of IL-1β or its receptor is protective against the development of adipose tissue inflammation. In this respect, a particularly interesting finding is that an IL-1β receptor antagonist has shown clinical effectiveness as a treatment for T2D (8, 9). Conversely, another cytokine, IL-18, increases in patients with obesity and insulin resistance, and the elevated levels strongly counteract obesity and metabolic syndrome (10–12).

Src homology region 2 domain-containing tyrosine phosphatase-2 (SHP2) is a ubiquitously expressed cytoplasmic protein tyrosine phosphatase encoded by the *PTPN11* gene in humans (13). This protein is expressed in all insulin-responsive tissues, including muscle (14), liver (15, 16), and adipose (17), as well as in the neurons that control energy regulation (18, 19). SHP2 was reported to play diverse roles in metabolic syndrome, and of interest here is the observation that animals with catalytically inactivating mutations in SHP2 display a strong reduction in adiposity and a pronounced resistance to diet-induced obesity and, therefore, have an overall better metabolic profile (20). Selective deletion of SHP2 in striated muscle results in insulin resistance, whereas liver-specific SHP2 knockout leads to less weight gain, decreased liver steatosis, and impeded development of insulin resistance in animals fed a high-fat diet (HFD) (14, 16). However, deletion of SHP2 from adipocytes does not significantly alter either systemic insulin sensitivity or glucose homeostasis (17). The expression of a dominant-active mutant (SHP2-D61A) in forebrain neurons of female transgenic mice confers resistance to HFD-induced obesity and liver steatosis and is accompanied by improved insulin sensitivity and glucose

This article contains supporting information.
‡These authors contributed equally to this work.
* For correspondence: Yang Sun, yangsun@nju.edu.cn; Qiang Xu, molpharm@163.com; Wenjie Guo, guowj@nju.edu.cn.

homeostasis (18). However, the role of SHP2 in macrophages is unclear, particularly concerning HFD-induced obesity, liver steatosis, and insulin sensitivity.

We previously reported that the knockout of macrophage SHP2 in mice (cSHP2-KO mice) led to elevated NLRP3 inflammasome activation, with increased levels of IL-1β and IL-18 and a resulting aggravation of murine peritonitis (21). However, in the present study, we observed an unexpected delay in body weight gain and an improvement in insulin resistance and hepatic steatosis in these cSHP2-KO mice when fed an HFD. We hypothesized that these improvements are because of an effect of IL-18. We confirmed this hypothesis using the following approaches: (i) use of an anti-IL-18 antibody treatment, which reversed insulin sensitivity and confirmed the predominant role of IL-18 in insulin sensitivity in the cSHP2-KO mice; (ii) generation of SHP2 and caspase-1 double KO (DKO) mice; these mice presented the same phenotype after HFD feeding as that observed in WT mice, indicating that the increase in IL-18 level caused by SHP2 knockout depends on caspase-1; and (iii) use of two SHP2-specific inhibitors, SHP099 and Phps1, which significantly ameliorated insulin resistance and hepatic steatosis. Our data provide new insights into the role of macrophagic SHP2 in metabolic disorders and suggest that SHP2 inhibition represents a new therapeutic strategy for the treatment of NAFLD.

Results

SHP2 deficiency in macrophages protects mice from HFD-induced obesity and insulin resistance

Obesity and inflammation are key contributors to insulin resistance and T2D. We investigated the role of macrophagic SHP2 in metabolism regulation by generating macrophage-specific conditional SHP2 knockout mice (cSHP2-KO), as described previously (21). When maintained on a normal chow diet (NCD), the cSHP2-KO mice did not show any obvious abnormal phenotype. However, when fed an HFD for 16 weeks, the cSHP2-KO mice showed considerably less body weight gain than WT counterparts (Fig. 1, *A* and *B*), although no significant difference was observed in food intake (Fig. 1*C*). After consuming the HFD for 14 weeks, all mice were subjected to metabolic cage studies. Significant enhancement of oxygen consumption and CO_2 production was observed in cSHP2-KO mice (Fig. 1, *D–F*), whereas no differences in heat production were observed between WT and cSHP2-KO mice in this study, suggesting that the lean phenotype of cSHP2-KO mice was mainly because of increased energy expenditure. In addition, intraperitoneal glucose tolerance (GTT) and insulin tolerance (ITT) tests were further performed to evaluate glucose homeostasis. The WT mice exhibited a much more severely impaired glucose metabolism and a more pronounced decrease in insulin sensitivity than the cSHP2-KO mice (Fig. 2, *A* and *B*). Because abnormally elevated hepatic gluconeogenesis also contributes to the overproduction of glucose in metabolic syndrome, we performed a pyruvate tolerance test (PTT) in mice after 16 weeks of HFD by intraperitoneally administering pyruvate, a precursor in the synthesis of glucose during gluconeogenesis. Results indicated that gluconeogenesis was significantly repressed in cSHP2-KO mice with HFD feeding (Fig. 2*C*), which was further confirmed by decreased mRNA expression of *Pepck* and *G6Pase* in liver (Fig. 2*D*), suggesting improved hepatic glucose metabolism. Hyperinsulinemia, suggestive of severe insulin resistance, was observed in the WT mice fed the HFD for 16 weeks. However, this hyperinsulinemia was partly suppressed by SHP2 knockout in macrophages (Fig. 2*E*), suggesting amelioration of insulin resistance in the cSHP2-KO mice.

Insulin signaling in the peripheral tissues, including liver, muscle, and fat, was also examined after injection of insulin via the portal vein. As shown in Fig. 2*F*, inhibited phosphorylation of AKT and GSK3β, indicating impaired insulin signaling, was significantly reversed in liver of cSHP2-KO mice. However, no significant difference in insulin signaling transduction was observed in muscle and adipose tissue of cSHP2-KO mice (Fig. S1).

SHP2 knockout in macrophages protects mice from HFD-induced hepatic steatosis

The occurrence of NAFLD in the setting of a high-fat diet has been well documented in previous studies (22). In our study, we found that the overall liver size and weight were noticeably smaller in the cSHP2-KO mice than in WT mice when both mouse types were fed an HFD (Fig. 3*A*). In line with this observation, hematoxylin and eosin (H&E) staining showed a significantly reduced accumulation of intrahepatic fat in the livers of the cSHP2-KO mice (Fig. 3*B*). The HFD-fed cSHP2-KO mice also showed a dramatic downregulation in the expression of caveolin-1, a lipid raft associated with lipid dynamics that has emerged as a key player in obesity and insulin resistance (23), indicating attenuated hepatic steatosis (Fig. 3*C*). Moreover, the serum and liver triglyceride (TG) levels were lower in the cSHP2-KO mice than in the WT mice (Fig. 3*D*). Phosphorylation of adenosine monophosphate activated protein kinase (AMPK) was also significantly increased in the livers of cSHP2-KO mice, indicating improved energy metabolism (Fig. 3*E*). To verify whether the amelioration of liver steatosis in cSHP2-KO mice is independent of liver injury, serum ALT and AST, which indicate liver injury, were detected, and no difference was observed between HFD-fed WT and cSHP2-KO mice (Fig. S2*A*). Moreover, the mRNA levels of hepatic TNFα and IL-6, two major proinflammatory cytokines, were also evaluated, and no difference was found (Fig. S2*B*).

We further characterized the improvement in the pathogenesis of hepatic steatosis in cSHP2-KO mice by examining the relative mRNA expression of the *fasn*, *srebp1c*, *ppar*γ, and *ppargc1*α genes. The expression of *srebp1c* was unaffected in the cSHP2-KO mice, but the expression of *fasn* was downregulated, whereas the expression of *ppar*γ and *ppargc1*α was upregulated in cSHP2-KO mice, indicating suppressed fat synthesis and enhanced energy metabolism (Fig. S3). Taken together, these findings suggest that the loss of SHP2 in macrophages results in resistance to HFD-induced metabolic disorders.

Loss of SHP2 in macrophages promotes IL-18 secretion and caspase-1 activation both in vivo and in vitro

Our previous studies revealed that the ablation of SHP2 in macrophages caused intensified pro-caspase-1 activation and led to overproduction of IL-1β and IL-18. In the present study,

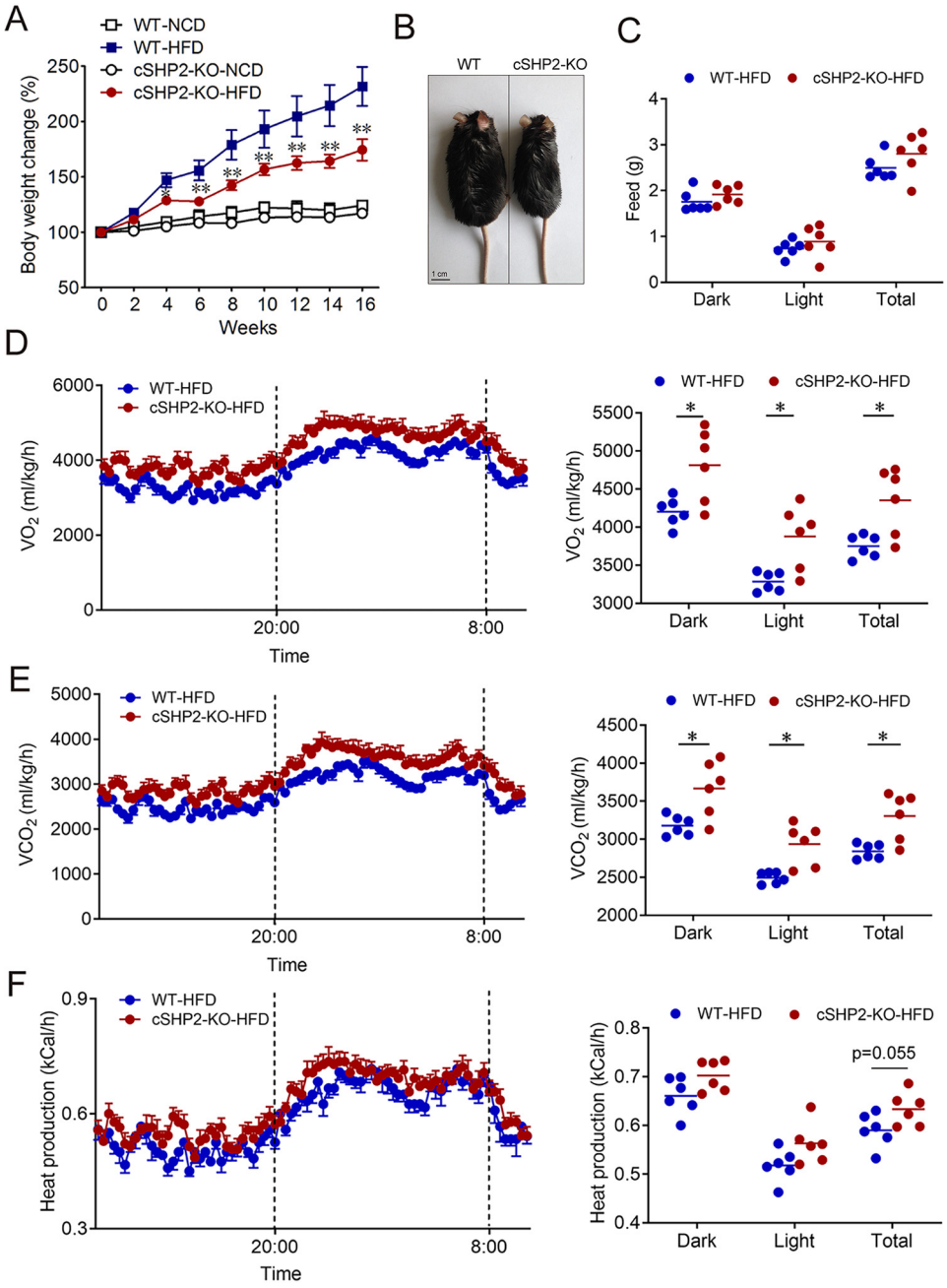

Figure 1. SHP2 deficiency in macrophages protects mice from HFD-induced obesity by promoting energy expenditure. WT and cSHP2-KO mice were fed on NCD or HFD. *A* to *C*, body weight change (*A* and *B*) and food intake (*C*) were recorded. **, $p < 0.01$ *versus* corresponding time point from WT-HFD. Energy expenditure of HFD-fed WT and cSHP2-KO mice were monitored using CLAMS for 24 h. *D*, the curve of oxygen consumption rate (VO_2). *E*, the carbon dioxide production rate (VCO_2). *F*, heat production. Data are expressed as mean ± S.E., $n = 6–8$. *, $p < 0.05$.

we also found that treatment with lipopolysaccharide (LPS) plus palmitic acid (PA) or ceramide (two stimuli that correspond to the status of an HFD) promoted the release of IL-18 and IL-1β and the activation of pro-caspase-1 in SHP2 KO macrophages compared with that of WT macrophages (Fig. 4, *C–F*). However, although elevation of IL-18 and IL-1β was observed in the serum of mice with HFD feeding, only IL-18 secretion was further elevated in cSHP2-KO mice (Fig. 4*A*). It should be noted that a high expression level of the IL-18 receptor (IL-18R) was observed in the liver tissue (Fig. S4), indicating that the IL-18/IL-18R pathway contributes to amelioration of liver steatosis in cSHP2-KO mice. Moreover, an increase in pro-caspase-1 activation was detected in peripheral macrophages (Fig. 4*B*). These results indicate that SHP2 negatively regulates pro-caspase-1 activation, and deletion of SHP2 in macrophages promotes IL-18 secretion both *in vitro* and *in vivo*.

IL-18 neutralization reverses the amelioration of HFD-induced metabolic syndrome in cSHP2-KO mice

Several studies have indicated that IL-18 strongly counteracts obesity and its related metabolic syndromes. However,

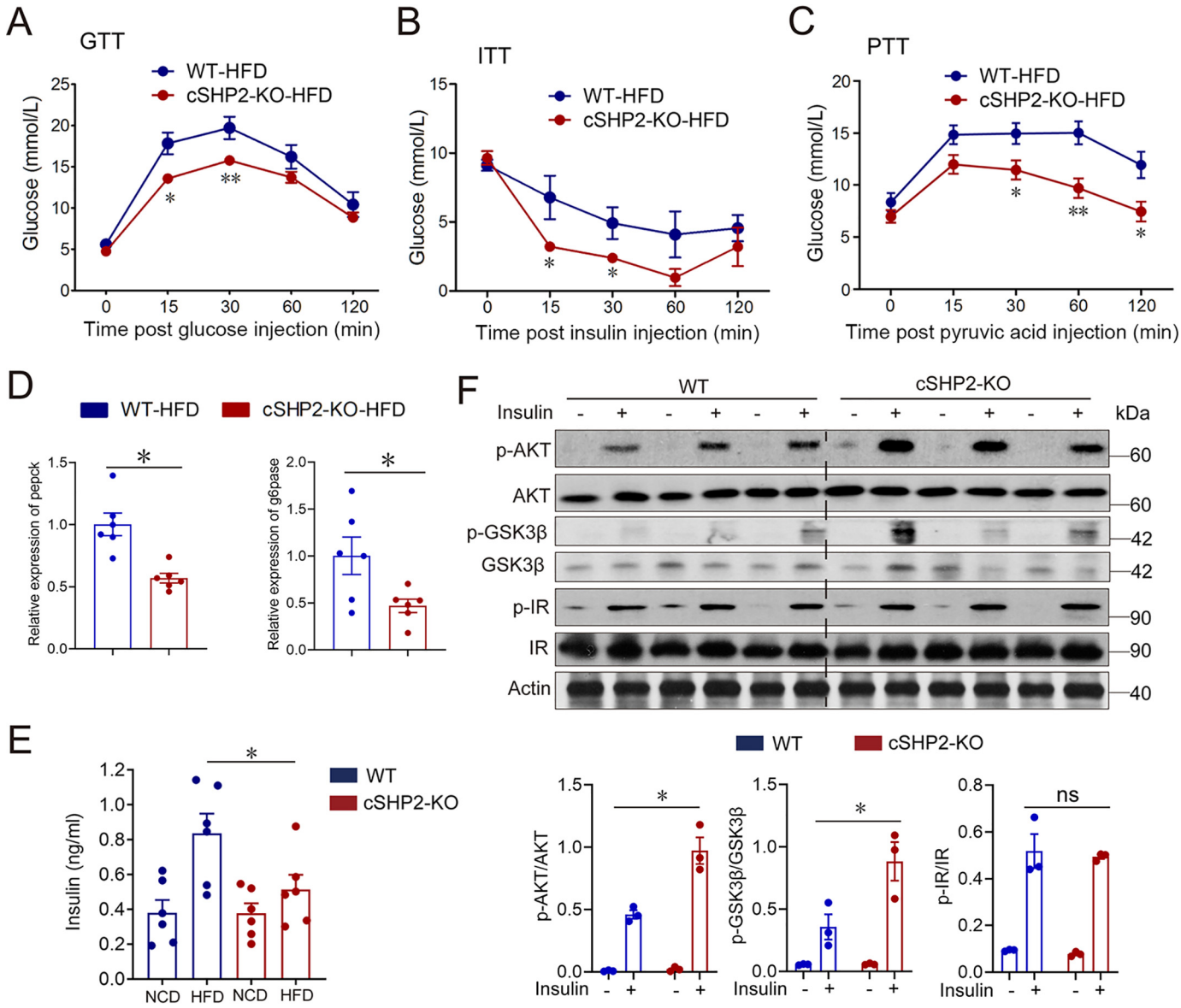

Figure 2. Ablation of SHP2 in macrophages protects mice from HFD-induced insulin resistance. WT and cSHP2-KO mice were fed on NCD or HFD. *A* and *B*, glucose tolerance test and insulin tolerance test were performed on mice with 14 weeks of HFD feeding. *C*, hepatic gluconeogenesis was determined by PTT assay. *, $p < 0.05$; **, $p < 0.01$ *versus* corresponding time point from WT. *D*, *Pepck* and *G6Pase* mRNA level in liver was determined by qPCR. *E*, fasting insulin level in the serum was determined by ELISA. *F*, insulin signaling in liver was determined by Western blot analysis after 6 h of fasting. Data are expressed as mean ± S.E., $n = 6–8$. *, $p < 0.05$; *ns*, not significant.

whether IL-18 is responsible for the alleviation of HFD-induced insulin resistance in cSHP2-KO mice remains unclear. Therefore, we investigated this hypothesis by conducting an IL-18 neutralization experiment. After being fed the HFD for 14 weeks, the cSHP2-KO mice were intraperitoneally administered 2.5 mg/kg anti-IL-18 antibody every other day a total of 5 times (anti-IgG was given as a control). This treatment resulted in a low circulating concentration of IL-18 (Fig. 5*A*). Consistent with previous data, the improvements in IPGTT and IPITT results normally observed in cSHP2-KO mice were significantly reversed by the anti-IL-18 administration (Fig. 5, *B* and *C*). Furthermore, the fasting serum insulin levels were markedly elevated in the cSHP2-KO mice administered the anti-IL-18 treatment (Fig. 5*D*). H&E-stained liver tissues showed considerably more inflammatory cell infiltration and more severe liver steatosis in the IL-18-neutralized than in anti-IgG-treated cSHP2-KO mice (Fig. 5*E*). Detection of liver insulin signaling also reflected a reversal of insulin sensitivity by IL-18 neutralization in cSHP2-KO mice, as indicated by a decrease in p-AKT (Ser473) levels after insulin stimulation (Fig. 5*F*). Energy metabolism was also significantly inhibited in the IL-18-neutralized cSHP2-KO mice, as indicated by suppressed p-AMPK expression (Fig. 5*G*). Previous studies have also suggested that IL-18 could promote lipid oxidation through AMPK activation in muscle while opposing lipid accumulation in adipose tissue (24). In this study, given that the primary phenotype was related to ameliorative insulin resistance and hepatic steatosis, we further evaluated the direct effect of IL-18 on hepatocytes. Results indicated that IL-18 could improve insulin sensitivity by alleviating the insulin-stimulated phosphorylation of AKT at Ser473,

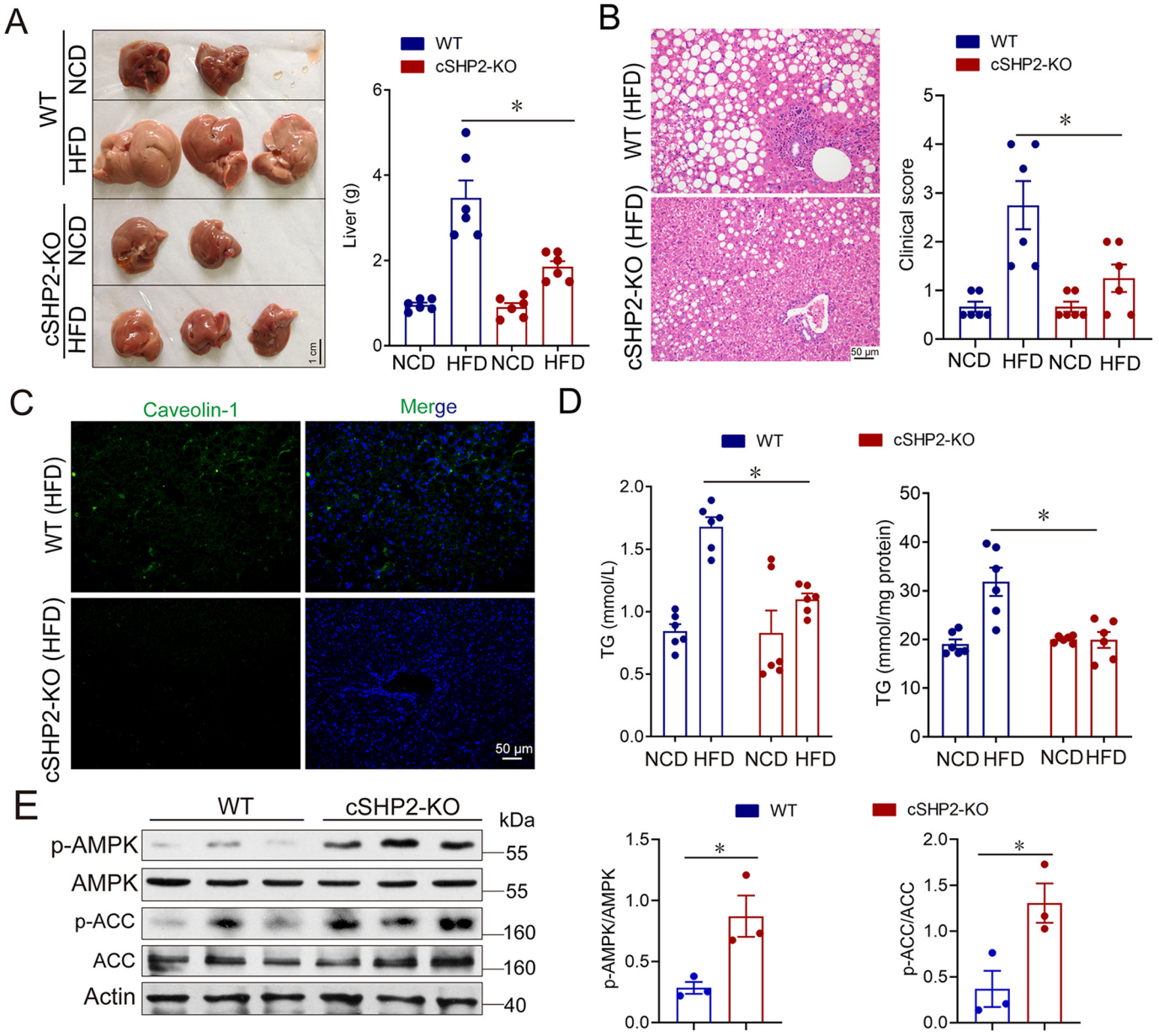

Figure 3. SHP2 deficiency in macrophages protects mice from HFD-induced hepatic steatosis. *A*, macroscopic appearance (*left*) and weight (*right*) of liver from WT and cSHP2-KO mice fed on NCD or HFD. *B* and *C*, H&E stain (*left*) and clinical score (*right*) (*B*) and caveolin-1 staining (*C*) of liver from WT and cSHP2-KO mice fed on HFD. *D*, TG in serum and liver from mice were measured. *E*, the expression of p-AMPK and p-ACC in liver of HFD mice was determined by Western blotting. Data are expressed as mean ± S.E. in *panels A*, *B*, and *D*, $n = 8–12$. *, $p < 0.05$.

which was inhibited by PA treatment (Fig. S5*A*). IL-18 also promoted the expression of p-AMPK and p-ACC in HepG2 cells treated with BSA or PA, reflecting improved energy metabolism (Fig. S5*B*). In our HFD-induced insulin resistance animal model, IL-18 was significantly elevated, whereas the increase in IL-1β in cSHP2-KO mice was not significant. We then wondered whether IL-18 opposes IL-1β's effect on insulin sensitivity. Thus, we assessed the role of IL-18 in IL-1β-induced insulin resistance and lipid generation using a liver cell model to address this question. We stimulated LPS-primed shRNA-Ctrl or shRNA-SHP2 THP-1 cells with palmitate and collected the supernatant (stimulated medium). Treatment of HepG2 cells with medium generated by shRNA-Ctrl THP-1 cells significantly inhibited insulin-induced AKT and GSK3β phosphorylation. However, shRNA-SHP2-stimulated medium significantly promoted insulin-induced AKT and GSK3β phosphorylation compared with shRNA-Ctrl-stimulated medium, reflecting an improvement in insulin sensitivity (Fig. S6*A*). PA treatment induced lipid accumulation and lipid synthesis-related gene expression in HepG2 cells, whereas IL-1β coordinated the effect of PA. IL-18 inhibited both PA and twice the level of IL-1β plus PA-induced lipid accumulation, TG generation, and the expression of *FASN*, *SREBP1A*, and *SREBP1C* (Fig. S6, *B–D*). Therefore, the effect of IL-18 on liver may at least partly contribute to the improved metabolic homeostasis observed in cSHP2-KO mice.

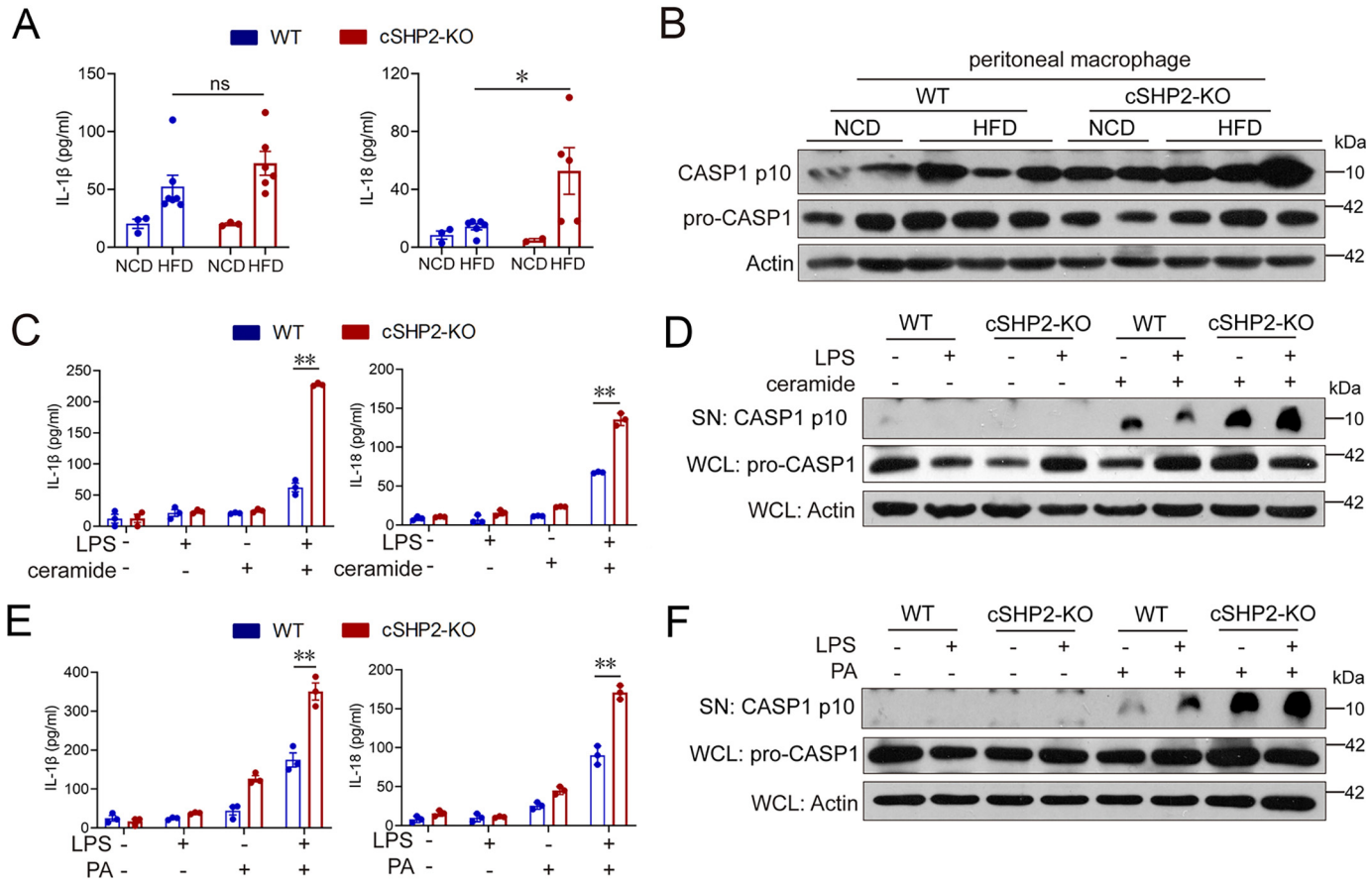

Figure 4. Loss of SHP2 in macrophages promotes elevated IL-18 secretion and caspase-1 activation both *in vivo* and *in vitro*. *A* and *B*, after feeding on NCD or HFD for 16 weeks, mice were sacrificed. The levels of IL-1β and IL-18 in the serum were determined by ELISA (*A*), and caspase-1 (CASP1) activation in peripheral macrophages from mice was determined by Western blotting (*B*). *C–F*, Peritoneal macrophages obtained from WT and cSHP2-KO mice were stimulated with 100 ng/ml LPS in the presence of ceramide (0.1 mM) or palmitic acid (*PA*, 200 μM). The level of IL-18 in the supernatant was determined by ELISA (*C* and *E*); CASP1 activation was determined by Western blotting (*D* and *F*). Data are expressed as mean ± S.E. in *panels A–E*, $n = 6$ in *A* and $n = 3$ in *C*, *E*. *, $p < 0.05$; **, $p < 0.01$.

Caspase-1 deficiency blocks the amelioration of HFD-induced insulin resistance and hepatic steatosis in cSHP2-KO mice

IL-18 is transcribed as a zymogen that requires cleavage. This is performed by caspase-1 to form the mature, active cytokine. Therefore, we also generated cSHP2 and caspase-1 double KO (DKO) mice by crossing cSHP2-KO mice with caspase-1 KO mice (Fig. S7). In these mice, both IL-1β and IL-18 generation was blocked by caspase-1 knockout (Fig. S8). The caspase-1 deficiency almost completely reversed the suppression of body weight increases in the cSHP2-KO mice (Fig. 6*A*). The GTT and ITT results were considerably worse from the DKO mice than from WT mice, suggesting a much greater impairment in glucose metabolism and a more pronounced decrease in insulin sensitivity (Fig. 6, *B* and *C*). Consistent with this, caspase-1 knockout significantly blocked the decrease of fasting insulin in the serum of cSHP2-KO mice (Fig. 6*D*). The basal phosphorylation of AKT and of IRβ in the liver was markedly higher in the DKO mice than in the cSHP2-KO mice, and no significant change was observed in the phosphorylation of AKT after insulin stimulation in the DKO mice (Fig. 6*E*). These data indicate severe impaired insulin signaling exists in DKO mice.

The amelioration of HFD-induced NAFLD by SHP2 deletion was also reversed by knockout of caspase-1. In particular, caspase-1 KO restored the macroscopic size, weight, and clinical scores of the livers of cSHP2-KO mice to levels similar to those of WT mice (Fig. 7, *A* and *B*). Notably, liver steatosis, as revealed by H&E and caveolin-1 staining, showed the same severity in both DKO and WT mice (Fig. 7, *B* and *C*). Further analysis of the serum and liver TG (Fig. 7*D*), low-density lipoprotein (LDL), and high-density lipoprotein (HDL) levels (Fig. S9, *A* and *B*) revealed a reversal of liver steatosis in the cSHP2-KO mice following caspase-1 knockout. The relative mRNA expression of *Fasn*, *Ppar*γ, and *Ppargc1*α also indicated a reversal of fat synthesis and energy metabolism in the DKO mice (Fig. S9*C*).

SHP2 inhibitors ameliorate metabolic disorders in HFD mice

We examined the relative expression of p-SHP2 in PA-treated murine bone marrow-derived macrophage (BMDM) and found that the SHP2 phosphorylation level was time-dependently enhanced with the treatment of PA (Fig. S10*A*). Moreover, we also collected peripheral blood mononuclear cells (PBMC) from healthy donors and diabetic patients. SHP2 phosphatase activity assay showed that SHP2 activity in PBMC from diabetic patients was significantly increased compared with healthy control (Fig. S10*B*). To further figure out whether

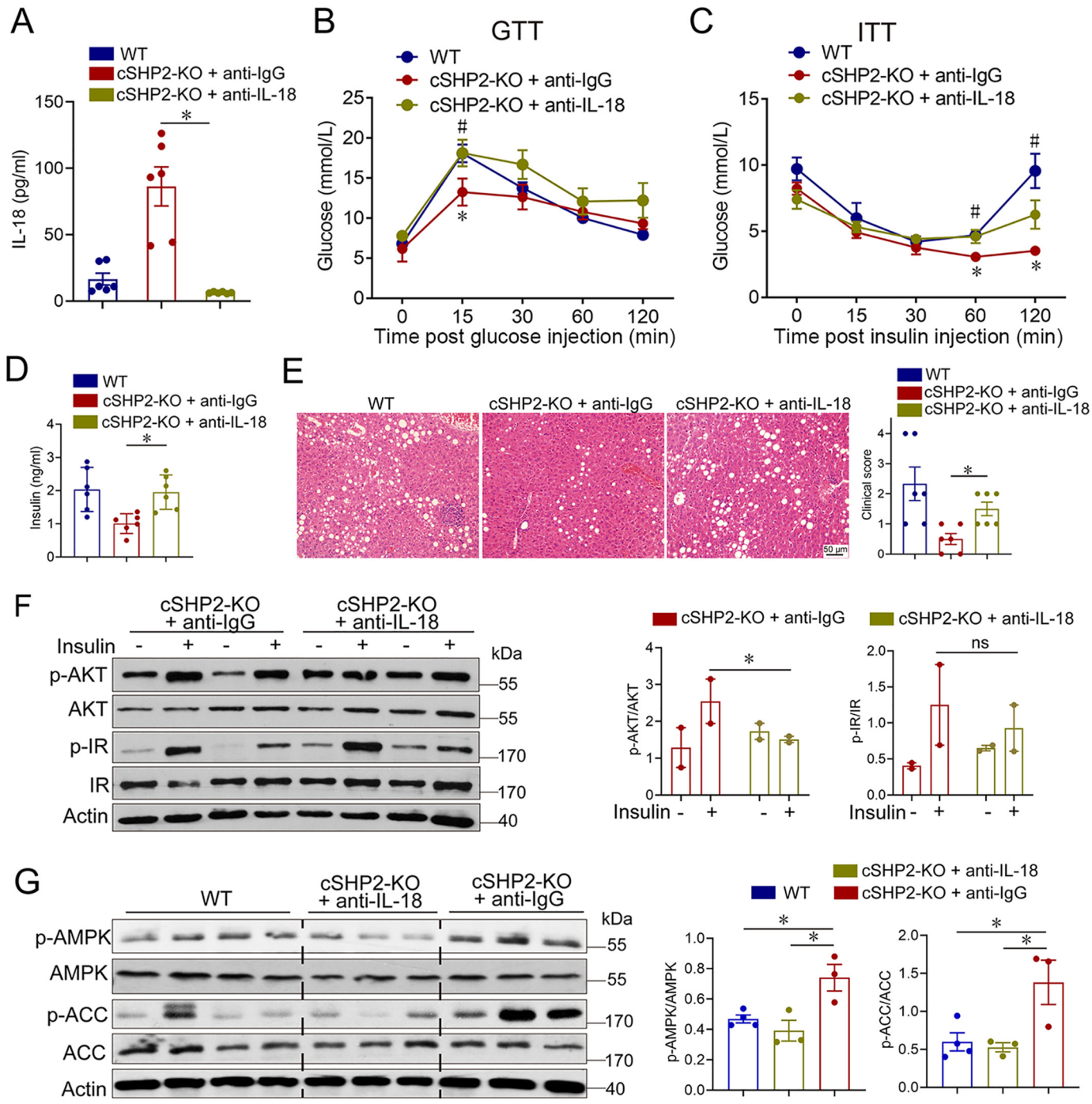

Figure 5. IL-18 neutralization reverses the amelioration of HFD-induced hepatic steatosis in cSHP2-KO mice. After feeding on HFD for 14 weeks, cSHP2-KO mice were intraperitoneally given 2.5 mg/kg anti-IL-18 every other day for 5 times (anti-IgG was given as control). *A*, IL-18 in serum of mice was determined by ELISA. *B* and *C*, glucose tolerance and insulin tolerance were determined by GTT and ITT assay. *D*, fasting insulin level in the serum was determined by ELISA. *E*, H&E stain (*left*) and clinical score (*right*) of liver from anti-IgG- or anti-IL-18-treated mice. *Scale bar*, 50 μm. *F*, insulin signaling in liver was determined by Western blotting after 6 h fasting. *G*, the expression of p-AMPK and p-ACC in liver were determined by Western blotting. Data are expressed as mean ± S.E. in *panels A–E*, $n = 6$. *, $p < 0.05$ *versus* WT; #, $P < 0.05$ *versus* cSHP2-KO+anti-IgG group in *panels A*, *B*, and *C* or as indicated in *panels E*, *F*, and *G*. *ns*, not significant.

macrophagic SHP2 is a potential drug target for controlling metabolic disorders, we treated HFD-fed WT male mice with two specific SHP2 inhibitors, SHP099 (25) and Phps1 (26). The mice were fed an HFD for 14 weeks and then given 2.5 and 5 mg/kg SHP099 i.p. for 16 days (5‰ DMSO was given as a control). As shown in Fig. 8*A*, no bodyweight changes occurred in response to the SHP099 treatment, but insulin sensitivity significantly improved after SHP099 treatment (Fig. 8*B* and *C*). The level of serum fasting insulin was significantly lower in the SHP099-treated mice than in the control mice (Fig. 8*D*).

The SHP099-induced improvements in insulin sensitivity may also be because of the promotion of IL-18 level (Fig. 8*E*).

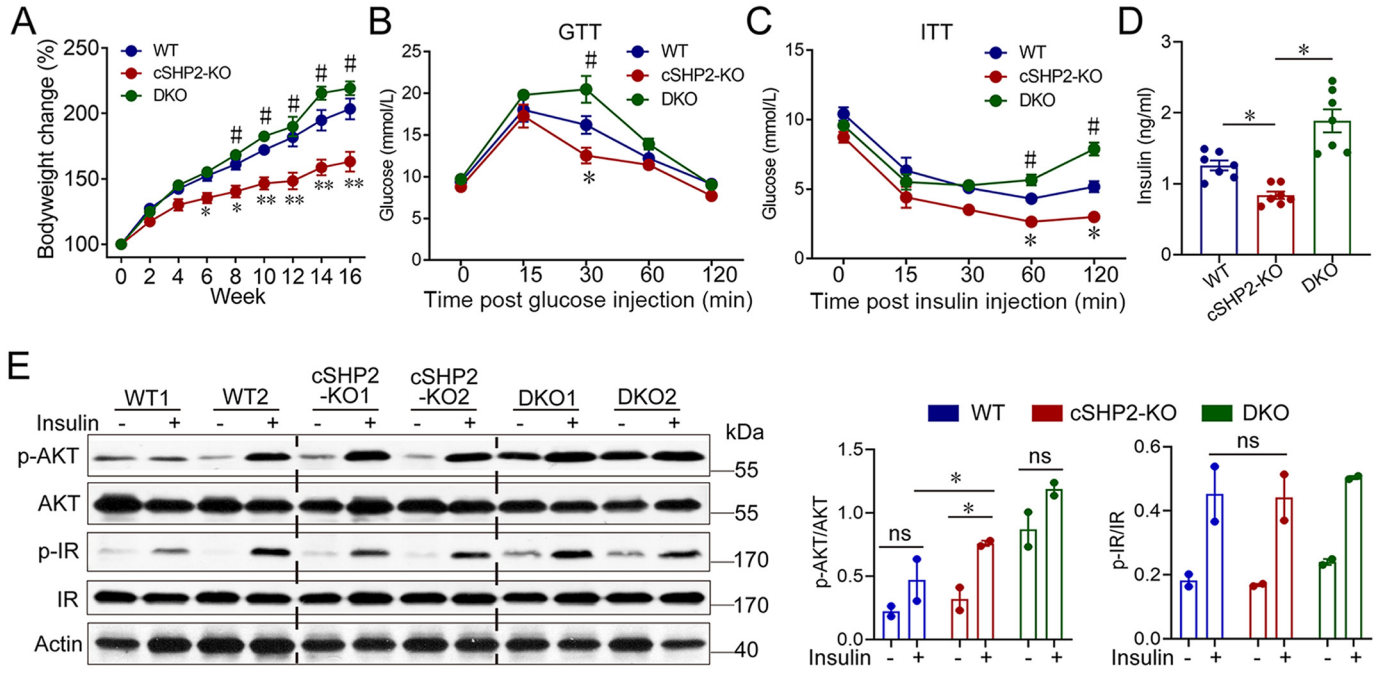

Figure 6. SHP2 deficiency-caused increase of insulin sensitivity is almost blocked by caspase-1 deletion. WT, cSHP2-KO, and SHP2/caspase-1 double knockout (DKO) mice were fed on HFD for 16 weeks. *A*, body weight change was recorded. *B* and *C*, GTT and ITT assays were carried out after mice were on HFD for 14 weeks. *D*, fasting insulin level in the serum of mice was determined by ELISA. *E*, insulin signaling in liver was determined by Western blotting after 6 h fasting. Data are expressed as mean ± S.E. in *panels A–E*, $n = 6$-8. *, $p < 0.05$; **, $p < 0.01$ *versus* WT; #, $P < 0.05$ *versus* cSHP2-KO in *panels A–C*. *, $p < 0.05$ *versus* values indicated in *panels D* and *E*. *ns*, not significant.

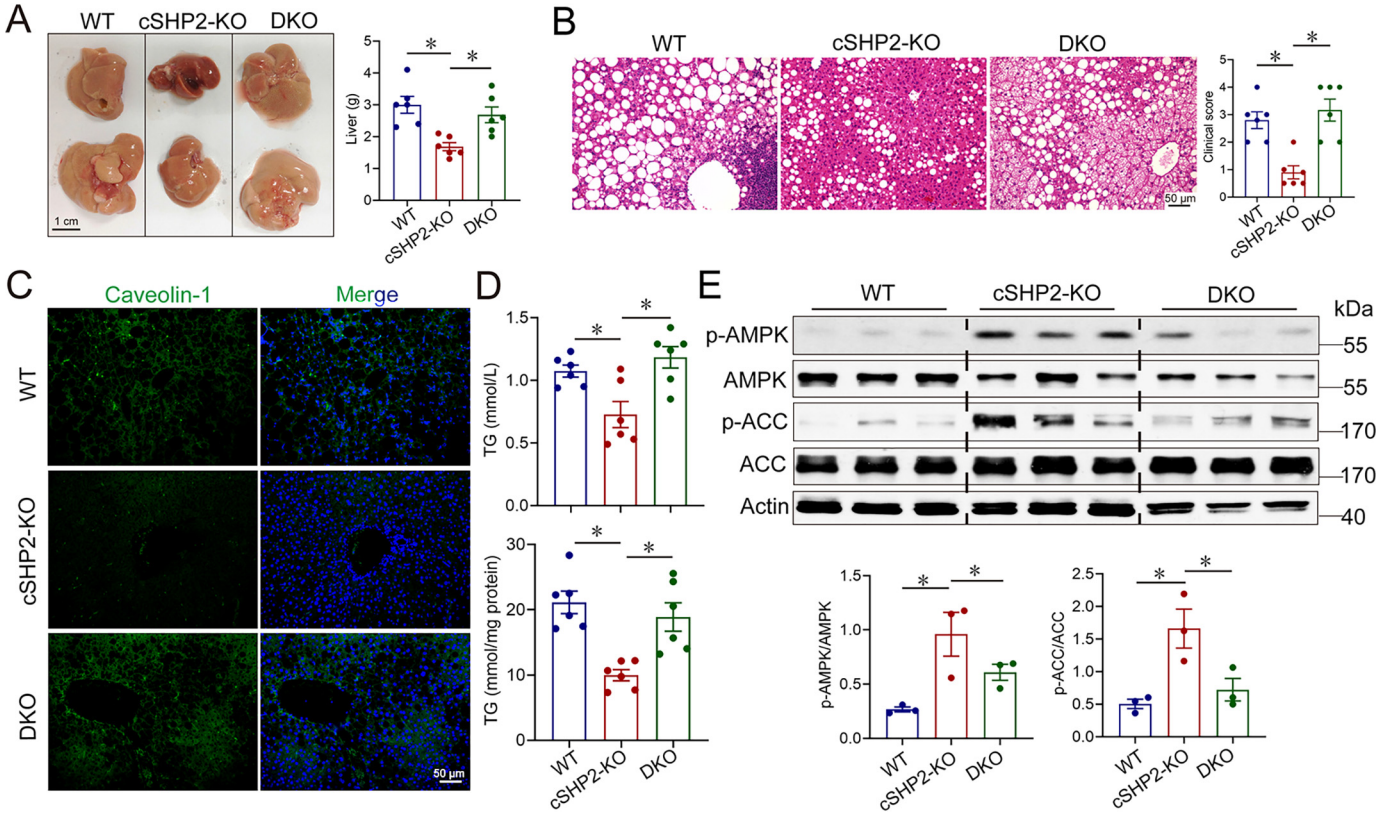

Figure 7. Caspase-1 deficiency reverses the amelioration of HFD-induced hepatic steatosis and insulin resistance in cSHP2-KO mice. After feeding on HFD for 16 weeks, mice were sacrificed. *A*, macroscopic appearance (*left*) and weight (*right*) of liver from mice. *B* and *C*, H&E stain (*left*), clinical score (*right*) (*B*) and caveolin-1 staining of liver from mice (*C*). *D*, TG in serum and liver were measured. *E*, the expression of p-AMPK and p-ACC in liver was determined by Western blotting. Data are expressed as mean ± S.E. in *panels A*, *B*, and *D*, $n = 6$. *, $p < 0.05$ *versus* indicated values.

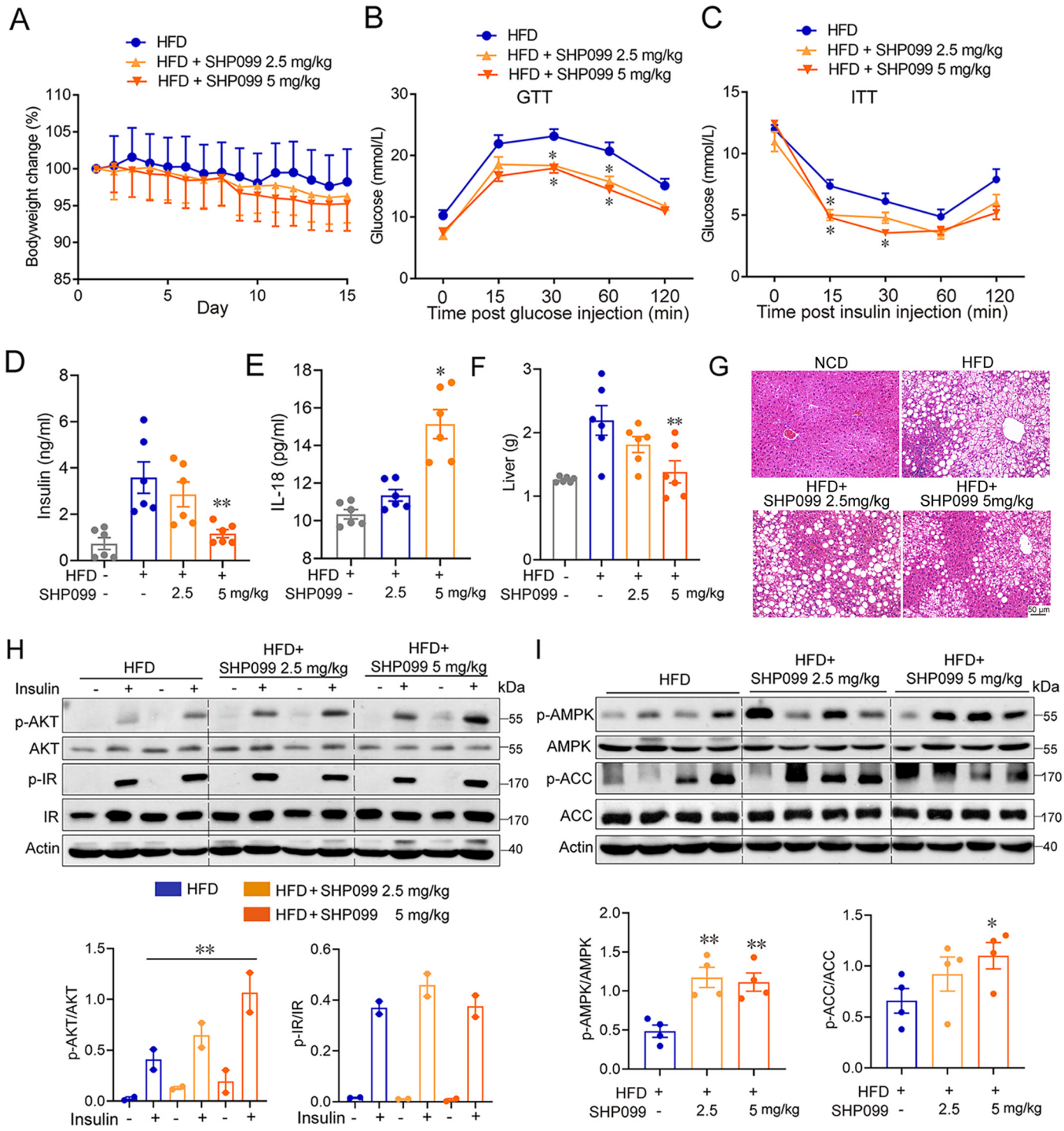

Figure 8. The SHP2 inhibitor SHP099 improved hepatic steatosis and insulin resistance in HFD mice. C57BL/6 mice were fed on HFD for 16 weeks. After that, mice were i.p. treated with 2.5 and 5 mg/kg SHP099 for 16 days. *A*, change of body weight was recorded. *B* and *C*, GTT and ITT assays were performed. *D* and *E*, fasting level of insulin and IL-18 in serum was examined by ELISA. *F* and *G*, weight (*F*) and H&E staining (*G*) of liver from SHP099-treated and control mice. *Scale bar*, 50 μm. *H*, the expression of p-AMPK and p-ACC in liver of SHP099-treated and control mice was determined by Western blotting. *I*, insulin signaling in liver was determined by Western blotting after 6 h of fasting. Data are expressed as mean ± S.E., $n = 6$. *, $p < 0.05$; **, $p < 0.01$ *versus* HFD or as indicated.

Upon sacrificing the mice, we observed an improvement in fatty liver in SHP099-treated mice compared with that of the control HFD-fed mice. The weight of the liver was significantly lower in the SHP099-treated mice (Fig. 8*F*), and H&E and caveolin-1 staining of the liver tissue showed an amelioration of HFD-induced liver steatosis by SHP099 treatment (Fig. 8*G* and Fig. S11). Liver insulin signaling detection suggested a reversal of insulin sensitivity by the SHP099 treatment, as indicated by an increment in p-AKT (Ser473) following insulin stimulation (Fig. 8*H*). Energy metabolism was also significantly improved,

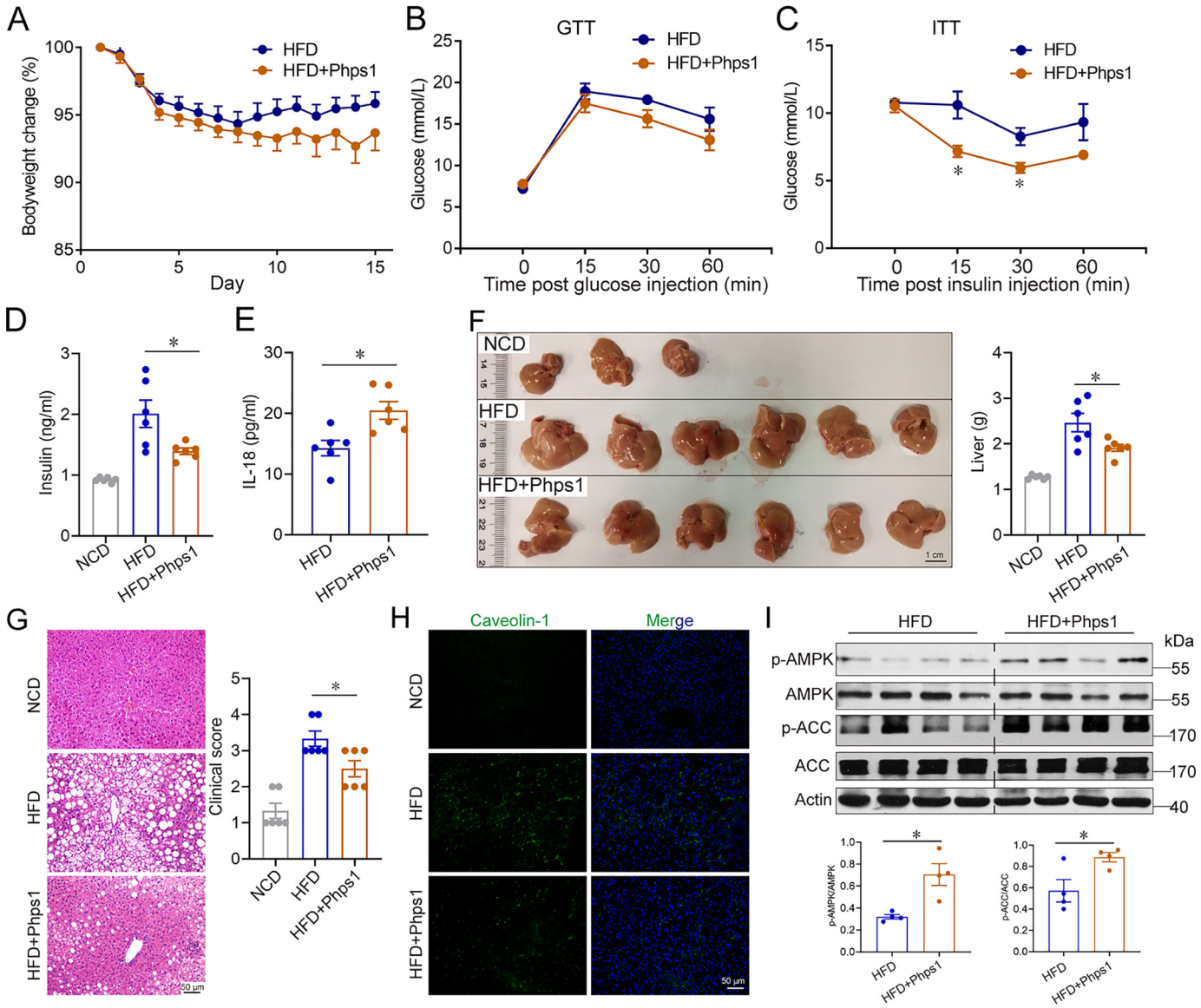

Figure 9. The SHP2 inhibitor Phps1 ameliorated hepatic steatosis and insulin resistance in HFD mice. C57BL/6 mice were fed on HFD for 16 weeks. After that, mice were i.p. treated with 2 mg/kg Phps1 for 16 days. *A*, change of body weight was recorded. *B* and *C*, GTT and ITT assays were performed. *D* and *E*, fasting level of insulin and IL-18 in serum was examined by ELISA. *F* and *G*, macroscopic appearance (*left*) and weight (*right*) (*F*) and H&E staining (*left*) and clinical score (*right*) (*G*) of liver from Phps1-treated and control mice. *Scale bar*, 50 μm. *H*, caveolin-1 expression in liver was determined by immunofluorescence stain. *I*, the expression of p-AMPK and p-ACC in liver of Phps1-treated and control mice were determined by Western blotting. Data are expressed as mean ± S.E., $n = 6$. *, $p < 0.05$ *versus* HFD or as indicated.

as indicated by elevated expression of p-AMPK and p-ACC in liver tissue (Fig. 8*I*).

The other SHP2 inhibitor, Phps1, was administered at 2 mg/kg i.p. for 16 days (5‰ DMSO was given as a control). Bodyweight and glucose metabolism were not influenced by Phps1 treatment, but insulin sensitivity was improved in the Phps1-treated mice (Fig. 9, *A–C*). The level of fasting insulin in the serum was significantly lower in the Phps1-treated mice than in the control mice (Fig. 9*D*). Phps1 treatment also increased the level of IL-18, whereas IL-1β was not affected (Fig. 9*E* and Fig. S12*A*). H&E and caveolin-1 staining of liver tissue showed an amelioration of HFD-induced liver steatosis by Phps1 treatment (Fig. 9, *F–H*). Phps1 treatment also promoted p-AMPK and p-ACC expression in liver tissue (Fig. 9*I*), reflecting an improved glucose metabolism. Additionally, Phps1 treatment caused a marked decrease in LDL level in both serum and liver; however, Phps1 treatment did not influence HDL expression (Fig. S12, *B* and *C*).

Discussion

Inflammation arising from the release of proinflammatory cytokines from infiltrating macrophages serves as an important contributor to the development of insulin resistance and related metabolic syndromes (3). The cytokines of the IL-1 family form one of the most important groups of inflammatory mediators. IL-1β is the most thoroughly studied member of this family and has been implicated in the pathogenesis of insulin action or secretion (7). In contrast, IL-18, another member of the same family, has been reported to counteract obesity and metabolic syndrome (10). Our previous study revealed that the ablation of SHP2 in macrophages caused an intensified NLRP3 activation and

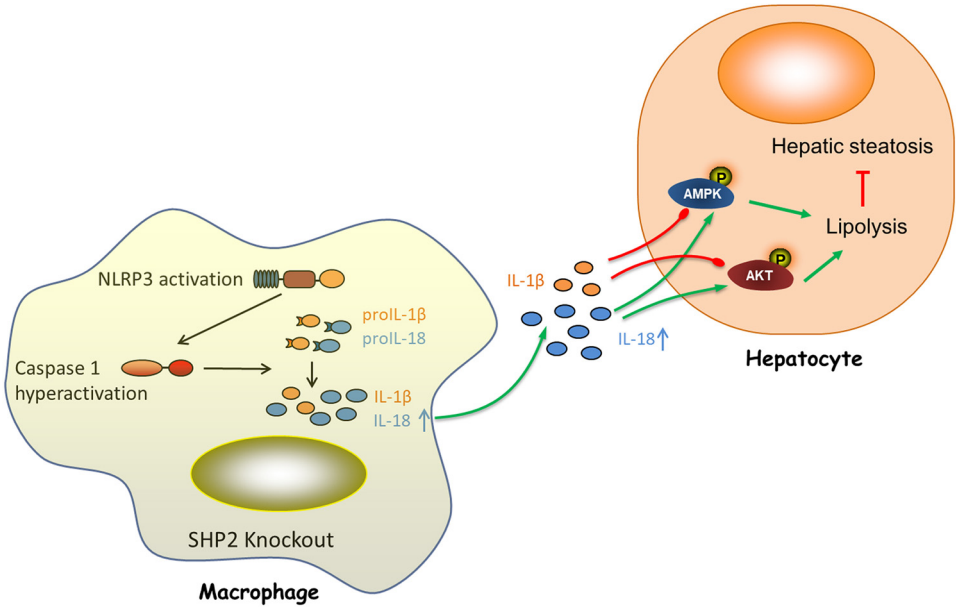

Figure 10. The graphic illustration for the mechanism of SHP2 regulating HFD-induced obesity and insulin resistance. Knockout of SHP2 in macrophage significantly ameliorates HFD-induced obesity and insulin resistance in mice through promoting caspase-1-dependent overproduction of IL-18. IL-18 promotes lipolysis in target tissues and alleviates the whole-body lipid accumulation as well as insulin resistance. More importantly, SHP2-specific inhibitor SHP099 and Phps1 significantly ameliorates HFD-induced insulin resistance and fat liver, indicating a potential drug target for treatment of insulin resistance.

overproduction of the proinflammatory IL-1β and IL-18. In the current study, we evaluated the effect of SHP2 deletion in macrophages on the development of metabolic syndrome (Fig. 10).

The release of IL-1β is triggered by NLRP3 inflammasome activation, a process that is believed to contribute to the development of both type 1 and type 2 diabetes (27). NLRP3 inflammasome-mediated IL-1β secretion has also been reported to contribute to adipose inflammation and insulin resistance (28, 29). Blocking of IL-1β signaling by an IL-1β receptor antagonist, by IL-1β receptor knockout, or by IL-1β neutralization may be effective strategies for the treatment of metabolic diseases, such as steatohepatitis and T2D (8).

Similarly, studies in mice on the loss of the NLRP3 inflammasome complex, NLRP3, ASC, and caspase-1, have also shown that NLRP3$^{-/-}$, ASC$^{-/-}$, and caspase-1$^{-/-}$ mice are resistant to HFD-induced obesity and exhibit high insulin sensitivity (30). Inhibition of NLRP3 inflammasome activation by several drugs also improves HFD-induced obesity and insulin resistance (31). Thus, inhibition of NLRP3 inflammasome activation is a potential avenue for the treatment of T2D.

However, IL-18 is also a product of NLRP3 inflammasome activation, and it plays a role opposite that of IL-1β with respect to obesity and insulin resistance. IL-18 receptor knockout mice show metabolic disorder, inflammation, and insulin resistance arising from mechanisms involving the activation of adenosine monophosphate activated protein kinase (AMPK) in skeletal muscle (24). Similarly, IL-18 knockout leads to obesity and insulin resistance (12, 32). Moreover, IL-18 may promote hepatic cell proliferation in rat liver regeneration (33). Mice lacking NLRP1 have defective lipolysis, which leads to metabolic syndrome, and these mice become obese because of IL-18 deficiency (11).

Our research here points out, for the first time, that mice lacking SHP2 in macrophages show resistance to obesity and improved insulin sensitivity, as well as reduced hepatic steatosis, and that these effects are dependent on IL-18 production, as indicated by the following evidence. The ablation of caspase-1 in cSHP2-KO mice completely reversed insulin sensitivity and reduced the extent of fatty liver, whereas IL-18 neutralization in cSHP2-KO mice showed the same effect as caspase-1 knockout. IL-18 could directly promote insulin sensitivity and AMPK activation in HepG2 cells. The SHP2 inhibitors SHP099 and Phps1 both ameliorated HFD-induced insulin resistance and hepatic steatosis.

Combined with our previous report that SHP2 is a negative regulator of NLRP3, we consider that SHP2 deletion resulted in IL-18 overproduction and that this response is partly caused by NLRP3 hyperactivation. However, this conclusion seems paradoxical in light of previous studies. This discrepancy may be partly caused by the difference in the expression of pro-IL-1β and pro-IL-18 under HFD treatment *in vivo*. Although IL-1β and IL-18 were both elevated after treatment with LPS plus PA *in vitro*, only the level of IL-18 in serum was higher in the cSHP2-KO mice (HFD fed) than in WT mice (HFD fed). The level of IL-1β was comparable between these two groups, although the levels in both groups were elevated compared with those in the NCD group. Unlike IL-1β, a cellular pool for IL-18 already exists before an inflammatory stimulus and is ready to be activated and released by the inflammasome (34). Another study also reported that IL-18 expression was increased and sustained after stimulation of TLRs, whereas IL-1β was induced but not sustained after chronic treatment (35). This may partly explain why the hyperactivation of the NLRP3 inflammasome in HFD mice after SHP2 knockout resulted in a higher increase in the level of IL-18.

Therapies that neutralize IL-1β, the major downstream product of inflammasome activation, have been tried as treatments for a number of metabolic diseases (36). However,

clinical experiments indicate that IL-1β plays a more prominent role in certain other diseases, such as gout and cardiovascular disease, than in obesity and T2D (37). An IL-1β receptor antagonist may also cause side effects, such as local injection site reactions and reduction in host defense against infection (9, 38). Thus, additional therapeutic treatments for obesity and T2D need to be explored. By discounting the usual view of the relationship between the NLRP3 inflammasome and T2D, our results imply that activating the NLRP3 inflammasome and selectively promoting IL-18 production is a new strategy for treatment of HFD-induced obesity and insulin resistance. However, because of the dual role of SHP2 in metabolic disease and insulin resistance in different tissues, the possibility of using SHP2 as a drug target remains to be determined. Two SHP2 inhibitors, Phps1 and SHP099, which act by different mechanisms, were employed in our study. Phps1 selectively inhibited SHP2 via binding the catalytic site of SHP2 (PTP domain) (26), whereas SHP099 inhibits SHP2 catalytic activity through allosteric stabilization of the inactive conformation of the enzyme (25, 39). Nevertheless, the findings reported here for Phps1 and SHP099 indicate that this strategy could promote insulin sensitivity and suppress hepatic steatosis in HFD mice.

Taken together, our findings reveal a novel association between SHP2 activation and insulin resistance and suggest that the selective promotion of IL-18 production through SHP2 inhibition is a promising avenue for attaining resistance to obesity and better insulin sensitivity.

Materials and methods

Chemicals, reagents, and antibodies

Sodium palmitate (PA), fatty acid-free BSA, phorbol myristate acetate (PMA), DAPI (RRID:AB_2629482), lipopolysaccharide (LPS), ceramide, and glucose were purchased from Sigma-Aldrich (St. Louis, MO). The SHP2 inhibitor PHPS1 was purchased from Calbiochem (La Jolla, CA). SHP099 hydrochloride (purity, >99%) was synthesized by Prof. Xiangbao Meng (School of Pharmaceutical Sciences, Peking University, Beijing, China) as previously described (40). Anti-p-Akt (4060, RRID:AB_10805010), anti-p-AMPK (2537), anti-p-IRβ (3024, RRID:AB_331253), anti-AMPK (5831, RRID:AB_10622186), anti-IR (3025, RRID:AB_2280448), and anti-caveolin-1 (3267, RRID:AB_2072166) were purchased from Cell Signaling Technology (Beverly, MA). Anti-CASP1 (ab108362, RRID:AB_10858984) and anti-p-SHP2 (ab62322, RRID:AB_945452) were purchased from Abcam (Cambridge UK). Anti-Akt (sc-8312, RRID:AB_671714) and anti-SHP2 (sc-7384, RRID:AB_628252) were purchased from Santa Cruz Biotechnology (Santa Cruz, CA). Anti-actin was purchased from Abmart (Shanghai, China). Anti-p-SHP2-PE (MA5-28045, RRID:AB_2745050) and Alexa Fluor 488 goat anti-rabbit IgG (A11008, RRID:AB_143165) were purchased from Invitrogen (Carlsbad, CA). High-fat diets (60 kcal% fat; no. 12492) were purchased from Research Diets (NJ, USA). RPMI 1640, fetal bovine serum (FBS), DMEM, and low-glucose DMEM were purchased from Life Technology (Carlsbad, CA). Human insulin (Novolin) for *in vivo* treatment was purchased from Novo Nordisk. All other chemicals were purchased from Sigma-Aldrich.

Mice

cSHP2-KO mice were generated by crossing $Shp2^{flox/flox}$ mice with lyz2-cre transgenic mice, as described previously (21). DKO mice were generated by crossing cSHP2-KO mice with caspase-1 KO mice. $SHP2^{flox/flox}$ littermates were used as control mice (WT mice). C57BL/6 mice (male, 10–12 weeks old, 23–25 g) were purchased from the Model Animal Research Center of Nanjing University (Nanjing, China). The animals were housed, five per cage with food and water *ad libitum*, on a 1-h light/dark cycle with lights on at 6:00 a.m. and controlled (22–23°C) temperature. Animal welfare and experimental procedures were carried out in strict accordance with the *Guide for the Care and Use of Laboratory Animals* (National Institutes of Health, USA) (41) and the related ethical regulations of our university. All efforts were made to minimize animals' suffering and to reduce the number of animals used. All studies involving animals are reported in accordance with the ARRIVE guidelines for reporting experiments involving animals (42, 43).

Cell culture

Bone marrow cells were isolated from C57BL/6 mice and cultured with DMEM supplemented with 10% fetal bovine serum (Invitrogen) and 20 ng/ml macrophage colony-stimulating factor (PeproTech, Rocky Hill, NJ). Culture fluid was exchanged for fresh culture medium every 3 days. Under these conditions, an adherent macrophage monolayer was obtained at day 7. Cells were seeded on 24-well plates. After culture for 6 h without macrophage colony-stimulating factor, the cells were used for the experiments as bone marrow-derived macrophages (BMDM). Peritoneal macrophages were harvested from C57BL/6 mouse peritoneal cavity and purified by adherence to tissue culture plastic. Human HepG2 cells were purchased from the Shanghai Institute of Cell Biology (Shanghai, China) and maintained in MEM supplemented with 100 units/ml of penicillin, 100 mg/ml of streptomycin, and 10% fetal calf serum under a humidified 5% (v/v) CO_2 atmosphere at 37 °C. 50 mM sodium palmitate was solubilized in PBS at 60 °C and then conjugated with 10% fatty acid-free BSA to achieve a final palmitate concentration of 5 mM. The conjugation was performed to increase the cell uptake of palmitate. The vehicle was 10% fatty acid-free BSA in medium.

ELISA analysis

Serum from mice in each group was taken, and the levels of insulin and cytokine were subjected to ELISA analysis by a commercial kit (IL-1β and IL-18 kits from Raybiotech and insulin kit from ALPCO).

Real-time PCR

Real-time PCR was performed as follows. RNA samples were reverse transcribed to cDNA and subjected to quantitative PCR, which was performed with the Bio-Rad CFX96 Touch™ real-time PCR detection system (Bio-Rad, Hercules, CA) using iQTM SYBR® Green supermix (Bio-Rad), and threshold cycle numbers were obtained using Bio-Rad CFX Manager software. The program for amplification was 1 cycle of 95 °C for 2 min,

followed by 40 cycles of 95 °C for 10 s, 60 °C for 30 s, and 95 °C for 10 s. The primer sequences used were the following: mouse IL-1β, forward, 5′-CCAAGCTTCCTTGTGCAAGTA-3′; reverse, 5′-AAGCCCAAAGTCCATCAGTGG-3′; mouse IL-18, forward, 5′-TGGTTCCATGCTTTCTGGACTCCT-3′; reverse, 5′-TTCCTGGGCCAAGAGGAAGTGATT-3′; mouse IL-6, forward, 5′-CTGCAAGAGACTTCCATCCAGTT-3′; reverse, 5′-GAAGTAGGGAAGGCCGTGG-3′; mouse TNFα, forward, 5′-CTGTAGCCCACGTCG TAGC-3′, reverse, 5′-TTGAGATCCATGCCGTTG-3′; mouse fasn, forward, 5′-TCCTGGAACGAGAACACGATCT-3′; reverse, 5′-GAGACGTGTCACTCCTGGACTTG-3′; mouse srebp1c, forward, 5′-CACGGAGCCATGGATTGC-3′; reverse, 5′-CCCGGGAAGTCACTGTCTTG-3′; mouse pparγ forward, 5′-CACGATGCTGTCCTCCTTGA-3′; reverse, 5′-GTGTGATAAAGCCATTGCCGT-3′; mouse ppargc1α, forward, 5′-ATACCGCAAAGAGCACGAAGAAG-3′; reverse, 5′-CTCAAGAGCAGCGAAAGCGTCACAG-3′; mouse actin, forward, 5′-GGCAAATTCAACGGCACA-3′; reverse, 5′-GTTAGTGGGGTCTCGCTCTG-3′; human fasn, forward, 5′-AGGTTTGATGCCTCCTTCTTCGGA-3′; reverse, 5′-TGGCTTCATAGGTGACTTCCAGCA-3′; human srebp1a, forward, 5′-TCAGCGAGGCGGCTTTGGAGCAG-3′; reverse, 5′-CATGTCTTCGATGTCGGTCAG-3′; human srebp1c, forward, 5′-GGAGGGGTAGGGCCAACGGCCT-3′; reverse, 5′-CATGTCTTCGAAAGTGCAATCC-3′; human actin, forward, 5′-CTGGAACGGTGAAGGTGACA-3′; reverse, 5′-AAGGGACTTCCTGTAACAATGCA-3′.

Western blotting

The protein lysates were separated by 10% SDS-PAGE and subsequently electrotransferred onto a polyvinylidene difluoride membrane (Millipore, Bedford, MA). The membrane was blocked with 5% nonfat milk for 1 h at room temperature. The blocked membrane was incubated with the indicated primary Abs and then with a horseradish peroxidase-conjugated secondary Ab. Protein bands were visualized using the Western blot detection system according to the manufacturer's instructions (Cell Signaling Technology, MA).

Metabolic studies

Male mice were fed either lean diet or an HFD (60% fat calories) for 14 weeks and had free access to water and food. Glucose tolerance test (GTT), insulin tolerance test (ITT), and pyruvate tolerance test (PTT) were conducted after mice were fed an HFD for 14 weeks. For GTT, the mice were fasted overnight (~12 h). The next morning, mice were injected intraperitoneally with glucose solution at a dosage of 1 g/kg body weight. For ITT, the mice were fasted for 4 h, and then mice were injected intraperitoneally with insulin solution at a dosage of 1 IU/kg. For PTT, mice were fasted for 6 h during the daytime, followed by i.p. injection of sodium pyruvate (2 g/kg). Blood glucose levels were measured using a FreeStyle Lite glucometer. For the metabolizable cage study, male mice fed with an HFD for 14 weeks were acclimatized in clams (Columbus Instruments) for 1 day, and VO_2, VCO_2, heat production, and feed were examined in the next 48 h.

Statistical analysis

Data are expressed as mean ± S.E. One-way analysis of variance (ANOVA) with Tukey *post hoc* test and two-way ANOVA was used for statistical evaluation. All statistical analyses were conducted using GraphPad Prism software, version 7.0 (GraphPad Software Inc., La Jolla, CA, RRID:SCR_002798). P values of <0.05 were considered statistically significant.

Study approval

All of the animal studies were approved by the Animal Ethical and Welfare Committee of Nanjing University. All human studies were approved by the ethics committee of Jiangsu Province Hospital. T2D patients were recruited by Jiangsu Province Hospital under protocol 2014-SR-003. Written informed consent was obtained from all subjects. The studies abide by the Declaration of Helsinki principles.

Data availability statement

All data are contained within the manuscript.

Acknowledgments—We thank Dr. Hongwen Zhou (the First Affiliated Hospital with Nanjing Medical University, China) for collecting clinical specimens.

Author contributions—W. L., Y. Y., and Y. Z. data curation; W. L., Y. Y., Y. Z., L. S., and J. G. formal analysis; W. L., M. W., T. F., and S. P. methodology; Y. Y., M. W., T. F., Y. Z., L. S., G. D., and W. G. investigation; X. M., L. K., and G.-S. F. resources; G.-S. F., Q. X., and Y. S. writing-review and editing; W. G. writing-original draft; Q. X. and Y. S. supervision; Q. X. and Y. S. funding acquisition.

Funding and additional information—This work was supported by National Natural Science Foundation of China (91853109, 81872877, 81730100, 81922067, 81673436, and 81970709), Open Fund of State Key Laboratory of Drug Research (SIMM1903KF-10), Fundamental Research Funds for the Central Universities (14380114, 14380128), and Mountain-Climbing Talents Project of Nanjing University.

Conflict of interest—The authors declare that they have no conflicts of interest with the contents of this article.

Abbreviations—The abbreviations used are: cSHP2-KO, conditional SHP2 knockout; SHP2, Src homology 2 domain-containing tyrosine phosphatase-2; T2D, type 2 diabetes; NAFLD, nonalcoholic fatty liver disease; NCD, normal chow diet; HFD, high-fat diet; DKO, double knockout; NLRP3, Nod-like receptor family protein 3; IPGTT, intraperitoneal glucose tolerance test; IPITT, intraperitoneal insulin tolerance test; AKT, protein kinase B; IRβ, insulin receptor β; AMPK, adenosine monophosphate activated protein kinase; LPS, lipopolysaccharide; PA, palmitic acid; LDL, low-density lipoprotein; HDL, high-density lipoprotein; BMDM, bone marrow-derived macrophage; PBMC, peripheral blood mononuclear cells; ANOVA, analysis of variance.

References

1. Xu, H. (2013) Obesity and metabolic inflammation. *Drug Discov. Today Dis. Mech.* **10,** 21–25 CrossRef
2. de Luca, C., and Olefsky, J. M. (2008) Inflammation and insulin resistance. *FEBS Lett.* **582,** 97–105 CrossRef Medline
3. Tack, C. J., Stienstra, R., Joosten, L. A., and Netea, M. G. (2012) Inflammation links excess fat to insulin resistance: the role of the interleukin-1 family. *Immunol. Rev.* **249,** 239–252 CrossRef Medline
4. Shoelson, S. E., Herrero, L., and Naaz, A. (2007) Obesity, inflammation, and insulin resistance. *Gastroenterology* **132,** 2169–2180 CrossRef
5. Donath, M. Y., and Shoelson, S. E. (2011) Type 2 diabetes as an inflammatory disease. *Nat. Rev. Immunol.* **11,** 98–107 CrossRef Medline
6. Spranger, J., Kroke, A., Mohlig, M., Hoffmann, K., Bergmann, M. M., Ristow, M., Boeing, H., and Pfeiffer, A. F. (2003) Inflammatory cytokines and the risk to develop type 2 diabetes: results of the prospective population-based European Prospective Investigation into Cancer and Nutrition (EPIC)-Potsdam Study. *Diabetes* **52,** 812–817 CrossRef
7. Jager, J., Gremeaux, T., Cormont, M., Le Marchand-Brustel, Y., and Tanti, J. F. (2007) Interleukin-1beta-induced insulin resistance in adipocytes through down-regulation of insulin receptor substrate-1 expression. *Endocrinology* **148,** 241–251 CrossRef Medline
8. Maedler, K., Dharmadhikari, G., Schumann, D. M., and Storling, J. (2009) Interleukin-1 beta targeted therapy for type 2 diabetes. *Expert Opin. Biol. Ther.* **9,** 1177–1188 CrossRef Medline
9. Larsen, C. M., Faulenbach, M., Vaag, A., Volund, A., Ehses, J. A., Seifert, B., Mandrup-Poulsen, T., and Donath, M. Y. (2007) Interleukin-1-receptor antagonist in type 2 diabetes mellitus. *N. Engl. J. Med.* **356,** 1517–1526 CrossRef
10. Yasuda, K., Nakanishi, K., and Tsutsui, H. (2019) Interleukin-18 in health and disease. *Int. J. Mol. Sci.* **20,** 649 CrossRef
11. Murphy, A. J., Kraakman, M. J., Kammoun, H. L., Dragoljevic, D., Lee, M. K., Lawlor, K. E., Wentworth, J. M., Vasanthakumar, A., Gerlic, M., Whitehead, L. W., DiRago, L., Cengia, L., Lane, R. M., Metcalf, D., Vince, J. E., *et al.* (2016) IL-18 production from the NLRP1 inflammasome prevents obesity and metabolic syndrome. *Cell Metab.* **23,** 155–164 CrossRef Medline
12. Zorrilla, E. P., and Conti, B. (2014) Interleukin-18 null mutation increases weight and food intake and reduces energy expenditure and lipid substrate utilization in high-fat diet fed mice. *Brain Behav. Immun.* **37,** 45–53 CrossRef Medline
13. Hof, P., Pluskey, S., Dhe-Paganon, S., Eck, M. J., and Shoelson, S. E. (1998) Crystal structure of the tyrosine phosphatase SHP-2. *Cell* **92,** 441–450 CrossRef Medline
14. Princen, F., Bard, E., Sheikh, F., Zhang, S. S., Wang, J., Zago, W. M., Wu, D., Trelles, R. D., Bailly-Maitre, B., Kahn, C. R., Chen, Y., Reed, J. C., Tong, G. G., Mercola, M., Chen, J., *et al.* (2009) Deletion of Shp2 tyrosine phosphatase in muscle leads to dilated cardiomyopathy, insulin resistance, and premature death. *Mol. Cell. Biol.* **29,** 378–388 CrossRef Medline
15. Matsuo, K., Delibegovic, M., Matsuo, I., Nagata, N., Liu, S., Bettaieb, A., Xi, Y., Araki, K., Yang, W., Kahn, B. B., Neel, B. G., and Haj, F. G. (2010) Altered glucose homeostasis in mice with liver-specific deletion of Src homology phosphatase 2. *J. Biol. Chem.* **285,** 39750–39758 CrossRef Medline
16. Nagata, N., Matsuo, K., Bettaieb, A., Bakke, J., Matsuo, I., Graham, J., Xi, Y., Liu, S., Tomilov, A., Tomilova, N., Gray, S., Jung, D. Y., Ramsey, J. J., Kim, J. K., Cortopassi, G., *et al.* (2012) Hepatic Src homology phosphatase 2 regulates energy balance in mice. *Endocrinology* **153,** 3158–3169 CrossRef Medline
17. Bettaieb, A., Matsuo, K., Matsuo, I., Nagata, N., Chahed, S., Liu, S., and Haj, F. G. (2011) Adipose-specific deletion of Src homology phosphatase 2 does not significantly alter systemic glucose homeostasis. *Metabolism* **60,** 1193–1201 CrossRef Medline
18. He, Z., Zhang, S. S., Meng, Q., Li, S., Zhu, H. H., Raquil, M. A., Alderson, N., Zhang, H., Wu, J., Rui, L., Cai, D., and Feng, G. S. (2012) Shp2 controls female body weight and energy balance by integrating leptin and estrogen signals. *Mol. Cell. Biol.* **32,** 1867–1878 CrossRef Medline
19. do Carmo, J. M., da Silva, A. A., Ebaady, S. E., Sessums, P. O., Abraham, R. S., Elmquist, J. K., Lowell, B. B., and Hall, J. E. (2014) Shp2 signaling in POMC neurons is important for leptin's actions on blood pressure, energy balance, and glucose regulation. *Am. J. Physiol. Regul. Integr. Comp. Physiol.* **307,** R1438–R1447 CrossRef Medline
20. Tajan, M., Batut, A., Cadoudal, T., Deleruyelle, S., Le Gonidec, S., Saint Laurent, C., Vomscheid, M., Wanecq, E., Treguer, K., De Rocca Serra-Nedelec, A., Vinel, C., Marques, M. A., Pozzo, J., Kunduzova, O., Salles, J. P., *et al.* (2014) LEOPARD syndrome-associated SHP2 mutation confers leanness and protection from diet-induced obesity. *Proc. Natl. Acad. Sci. U S A* **111,** E4494–E4503 CrossRef Medline
21. Guo, W., Liu, W., Chen, Z., Gu, Y., Peng, S., Shen, L., Shen, Y., Wang, X., Feng, G. S., Sun, Y., and Xu, Q. (2017) Tyrosine phosphatase SHP2 negatively regulates NLRP3 inflammasome activation via ANT1-dependent mitochondrial homeostasis. *Nat. Commun.* **8,** 2168 CrossRef Medline
22. Lakhani, H. V., Sharma, D., Dodrill, M. W., Nawab, A., Sharma, N., Cottrill, C. L., Shapiro, J. I., and Sodhi, K. (2018) Phenotypic alteration of hepatocytes in non-alcoholic fatty liver disease. *Int. J. Med. Sci.* **15,** 1591–1599 CrossRef Medline
23. Fruhbeck, G., Lopez, M., and Dieguez, C. (2007) Role of caveolins in body weight and insulin resistance regulation. *Trends Endocrinol. Metab.* **18,** 177–182 CrossRef
24. Lindegaard, B., Matthews, V. B., Brandt, C., Hojman, P., Allen, T. L., Estevez, E., Watt, M. J., Bruce, C. R., Mortensen, O. H., Syberg, S., Rudnicka, C., Abildgaard, J., Pilegaard, H., Hidalgo, J., Ditlevsen, S., *et al.* (2013) Interleukin-18 activates skeletal muscle AMPK and reduces weight gain and insulin resistance in mice. *Diabetes* **62,** 3064–3074 CrossRef Medline
25. Chen, Y. N., LaMarche, M. J., Chan, H. M., Fekkes, P., Garcia-Fortanet, J., Acker, M. G., Antonakos, B., Chen, C. H., Chen, Z., Cooke, V. G., Dobson, J. R., Deng, Z., Fei, F., Firestone, B., Fodor, M., *et al.* (2016) Allosteric inhibition of SHP2 phosphatase inhibits cancers driven by receptor tyrosine kinases. *Nature* **535,** 148–152 CrossRef Medline
26. Hellmuth, K., Grosskopf, S., Lum, C. T., Wurtele, M., Roder, N., von Kries, J. P., Rosario, M., Rademann, J., and Birchmeier, W. (2008) Specific inhibitors of the protein tyrosine phosphatase Shp2 identified by high-throughput docking. *Proc. Natl. Acad. Sci. U S A* **105,** 7275–7280 CrossRef Medline
27. Masters, S. L., Dunne, A., Subramanian, S. L., Hull, R. L., Tannahill, G. M., Sharp, F. A., Becker, C., Franchi, L., Yoshihara, E., Chen, Z., Mullooly, N., Mielke, L. A., Harris, J., Coll, R. C., Mills, K. H., *et al.* (2010) Activation of the NLRP3 inflammasome by islet amyloid polypeptide provides a mechanism for enhanced IL-1beta in type 2 diabetes. *Nat. Immunol.* **11,** 897–904 CrossRef Medline
28. Tilg, H., Moschen, A. R., and Szabo, G. (2016) Interleukin-1 and inflammasomes in alcoholic liver disease/acute alcoholic hepatitis and nonalcoholic fatty liver disease/nonalcoholic steatohepatitis. *Hepatology* **64,** 955–965 CrossRef Medline
29. Finucane, O. M., Lyons, C. L., Murphy, A. M., Reynolds, C. M., Klinger, R., Healy, N. P., Cooke, A. A., Coll, R. C., McAllan, L., Nilaweera, K. N., O'Reilly, M. E., Tierney, A. C., Morine, M. J., Alcala-Diaz, J. F., Lopez-Miranda, J., *et al.* (2015) Monounsaturated fatty acid-enriched high-fat diets impede adipose NLRP3 inflammasome-mediated IL-1beta secretion and insulin resistance despite obesity. *Diabetes* **64,** 2116–2128 CrossRef Medline
30. Stienstra, R., van Diepen, J. A., Tack, C. J., Zaki, M. H., van de Veerdonk, F. L., Perera, D., Neale, G. A., Hooiveld, G. J., Hijmans, A., Vroegrijk, I., van den Berg, S., Romijn, J., Rensen, P. C., Joosten, L. A., Netea, M. G., *et al.* (2011) Inflammasome is a central player in the induction of obesity and insulin resistance. *Proc. Natl. Acad. Sci. U S A* **108,** 15324–15329 CrossRef Medline
31. Mridha, A. R., Wree, A., Robertson, A. A. B., Yeh, M. M., Johnson, C. D., Van Rooyen, D. M., Haczeyni, F., Teoh, N. C., Savard, C., Ioannou, G. N., Masters, S. L., Schroder, K., Cooper, M. A., Feldstein, A. E., and Farrell, G. C. (2017) NLRP3 inflammasome blockade reduces liver inflammation and fibrosis in experimental NASH in mice. *J. Hepatol.* **66,** 1037–1046 CrossRef Medline
32. Netea, M. G., Joosten, L. A., Lewis, E., Jensen, D. R., Voshol, P. J., Kullberg, B. J., Tack, C. J., van Krieken, H., Kim, S. H., Stalenhoef, A. F., van de Loo,

F. A., Verschueren, I., Pulawa, L., Akira, S., Eckel, R. H., *et al.* (2006) Deficiency of interleukin-18 in mice leads to hyperphagia, obesity and insulin resistance. *Nat. Med.* **12,** 650–656 CrossRef Medline

33. Zhang, J., Ma, C., Liu, Y., Yang, G., Jiang, Y., and Xu, C. (2014) Interleukin 18 accelerates the hepatic cell proliferation in rat liver regeneration after partial hepatectomy. *Gene* **537,** 230–237 CrossRef
34. Kupz, A., Guarda, G., Gebhardt, T., Sander, L. E., Short, K. R., Diavatopoulos, D. A., Wijburg, O. L., Cao, H., Waithman, J. C., Chen, W., Fernandez-Ruiz, D., Whitney, P. G., Heath, W. R., Curtiss, R., 3rd, Tschopp, J., *et al.* (2012) NLRC4 inflammasomes in dendritic cells regulate noncognate effector function by memory CD8(+) T cells. *Nat. Immunol.* **13,** 162–169 CrossRef Medline
35. Zhu, Q., and Kanneganti, T. D. (2017) Cutting edge: distinct regulatory mechanisms control proinflammatory cytokines IL-18 and IL-1beta. *J. Immunol.* **198,** 4210–4215 CrossRef Medline
36. Gabay, C., Lamacchia, C., and Palmer, G. (2010) IL-1 pathways in inflammation and human diseases. *Nat. Rev. Rheumatol.* **6,** 232–241 CrossRef Medline
37. Bhaskar, V., Yin, J., Mirza, A. M., Phan, D., Vanegas, S., Issafras, H., Michelson, K., Hunter, J. J., and Kantak, S. S. (2011) Monoclonal antibodies targeting IL-1 beta reduce biomarkers of atherosclerosis in vitro and inhibit atherosclerotic plaque formation in Apolipoprotein E-deficient mice. *Atherosclerosis* **216,** 313–320 CrossRef Medline
38. Kaiser, C., Knight, A., Nordstrom, D., Pettersson, T., Fransson, J., Florin-Robertsson, E., and Pilstrom, B. (2012) Injection-site reactions upon Kineret (anakinra) administration: experiences and explanations. *Rheumatol. Int.* **32,** 295–299 CrossRef Medline
39. Garcia Fortanet, J., Chen, C. H., Chen, Y. N., Chen, Z., Deng, Z., Firestone, B., Fekkes, P., Fodor, M., Fortin, P. D., Fridrich, C., Grunenfelder, D., Ho, S., Kang, Z. B., Karki, R., Kato, M., *et al.* (2016) Allosteric inhibition of SHP2: identification of a potent, selective, and orally efficacious phosphatase inhibitor. *J. Med. Chem.* **59,** 7773–7782 CrossRef Medline
40. Zhao, M., Guo, W., Wu, Y., Yang, C., Zhong, L., Deng, G., Zhu, Y., Liu, W., Gu, Y., Lu, Y., Kong, L., Meng, X., Xu, Q., and Sun, Y. (2019) SHP2 inhibition triggers anti-tumor immunity and synergizes with PD-1 blockade. *Acta Pharm. Sin. B* **9,** 304–315 CrossRef Medline
41. National Research Council. (2011) *Guide for the care and use of laboratory animals*, 8th ed., National Academies Press, Washington, D.C.
42. Kilkenny, C., Browne, W., Cuthill, I. C., Emerson, M., and Altman, D. G, NC3Rs Reporting Guidelines Working Group. (2010) Animal research: reporting in vivo experiments: the ARRIVE guidelines. *Br. J. Pharmacol.* **160,** 1577–1579 CrossRef Medline
43. McGrath, J. C., Drummond, G. B., McLachlan, E. M., Kilkenny, C., and Wainwright, C. L. (2010) Guidelines for reporting experiments involving animals: the ARRIVE guidelines. *Br. J. Pharmacol.* **160,** 1573–1576 CrossRef Medline